TEMPORAL AND SPATIAL CHANGE DETECTION OF ECOLOGICAL ENVIRONMENT QUALITY IN SHANXI PROVINCE BASED ON REMOTE SENSING

Sijia Wang[1], Yan Song[1234*], Wenjun Qin[1], Yuhong Tu[1], Beibei Li[1], Zhijie Zhang[2]

[1] School of Geography and Information Engineering, China University of Geosciences (Wuhan), Wuhan, China – songyan@cug.edu.cn

[2] School of Public Administration, China University of Geosciences (Wuhan), Wuhan, China – songyan@cug.edu.cn

[3] Key Laboratory of Geological Survey and Evaluation of Ministry of Education, China University of Geosciences (Wuhan), Wuhan, China – songyan@cug.edu.cn

[4] National Engineering Research Center of Geographic Information System, China University of Geosciences (Wuhan), Wuhan, China – songyan@cug.edu.cn

KEY WORDS: Ecological environment quality; Geodetector; Spatial autocorrelation; PCA; RSEI

ABSTRACT:

Long term coal mining produces pollutants such as coal gangue, coal mine gas and mine water. With the rapid urbanization, the increased environmental burden has led to the deterioration of environmental pollution problems, which seriously restricts the harmonious and sustainable development of the ecological economy. In order to understand the changes of the ecological environment in Shanxi Province in the past seven years, this paper selects the ground remote sensing data of Shanxi Province in the winter of 2013-2019 to obtain remote sensing ecological indicators (RSEI) that comprehensively reflect the ground ecological status, and uses spatial autocorrelation and geological detectors to explore the driving factors of the ecological environment differences in Shanxi Province, revealing the dynamic mechanism of the RSEI differences in Shanxi Province. The results show that the overall ecological environment quality in winter in Shanxi Province has a downward trend from 2013 to 2017 and an upward trend from 2018 to 2019. The spatial distribution of ecological environment quality between 2013 and 2019 is positively correlated. The clustering and outlier analysis chart of RSEI shows that in the seven years from 2013 to 2019, there are stable high value clusters in the north of Shanxi Province, while there are more low value clusters in the south. The significance test results show that the output value of the primary industry and the output value of the secondary industry dominated from 2013 to 2019.

1. INTRODUCTION

Energy security is an important issue in the world today. As an oil-poor country, China's energy structure of "more coal, less oil and less gas" determines the important position of coal in the energy structure. Coal is China's basic energy and important raw materials. In 2019, the national raw coal output accounted for 68.6% of the total disposable energy in the country. Coal has made an important contribution to ensuring the rapid economic and social development of China. Shanxi Province is rich in mineral resources and has exported coal resources to the country for a long time. However, coal mining produces pollutants such as coal gangue, coal mine gas and mine water, which will also cause surface subsidence and soil erosion. Under the background of rapid changes in the ecological environment, environmental problems such as soil pollution, air pollution and water pollution are getting worse and worse, seriously restricting the harmonious and sustainable development of the ecological economy. Remote sensing is different from the traditional field survey method and has the characteristics of multi-scale, multi temporal and large-scale observation. With the progress of remote sensing technology, the timeliness, availability and effectiveness of remote sensing data have been greatly improved. Ecological monitoring based on ecological parameters retrieved from remote sensing has become a hot research topic for scholars.

There are various ecosystems, and the technology of dynamic monitoring of ecological quality based on remote sensing has experienced a development process from simple to complex, from one-sided to comprehensive. Early scholars proposed single indicator evaluation method based on remote sensing to monitor the ecological environment, for example, the normalized difference vegetation index (NDVI) is used to monitor vegetation growth (KAUFMAN and TANRE, 1992; Lu et al., 2016); The modified normalized difference water index (MNDWI) (Singh et al., 2015) is used to extract the range of water bodies, and can be used to monitor the changes of water borders between years (Gao, 1996; Xu, 2006); The Forel-Ule Index (FUI) (Garaba et al., 2015) is an important indicator of the water quality, and is related to the water cleanliness and eutrophication status; The Land surface temperature (LST) (Yang et al., 2016), as a substitute of the surface temperature, is used to retrieve the surface thermal environment, which indirectly solves the deviation in the remote sensing estimation of the surface temperature, and is widely used in the urban heat island effect.

With the further understanding of the ecosystem, scholars found that the ecological indicators based on remote sensing retrieval reflect the changes of single aspect of the ecosystem in time and space. Therefore, single indicator ecological quality monitoring cannot reflect the spatio-temporal changes of the whole ecosystem (Xu et al., 2019). Canadian Statistician David J. Rapport and Tony Friend put forward the Pressure State Response (PSR) model in 1979. This model comprehensively considers environmental pressure, environmental state and social response indicators, and is widely used in the field of ecosystem evaluation. For example, the ecological environment

* Corresponding author.

status index (EI), the Scaled Drought Condition Index(SDCI) (Rhee et al., 2010), the Aggregate Drought Index (ADI) (Keyantash and Dracup, 2004) and MODIS Global Disturbance Index(MGDI) (Mildrexler et al., 2009). The comprehensive ecological assessment model can more comprehensively reflect the ecological statuses studied. However, the PSR model couples multiple indicators through the weighting method, and the determination of weights is entirely based on expert experience. Therefore, the comprehensive indicators generated through this process have the shortcomings of arbitrariness and subjectivity. Xu (Xu et al., 2018) proposed that the use of principal component analysis (PCA) can avoid the risk of artificially determining weights, which is more objective than the analytic hierarchy process (AHP), and uses PCA to couple the four indicators of greenness, humidity, dryness, and heat to generate Risk-Screening Environmental Indicators (RSEI) completely based on remote sensing data. The application of this index to evaluate the ecological status of Fuzhou, China, shows that RSEI can effectively reflect the regional ecological quality. In addition, RSEI is completely based on remote sensing data, which is characterized by rich data and easy access and excluding subjective weight setting. It is widely used in watershed (Li et al., 2022; Yang et al., 2021), plain (Ren et al., 2022), city (Hang et al., 2020; Tang et al., 2021), oasis (Gao et al., 2020) and other regions.

Xu (Xu et al., 2019) uses the sharpened surface temperature image to improve RSEI, Specifically, he monitors the ecological changes in Fujian Province, China, from 2002 to 2017 by generating the RSEI time series that reflect the ecological status, and conducting spatial autocorrelation and change vector analysis on the time series. Yue (Yue et al., 2019) observed the ecological quality changes of 35 major cities in China by using the RSEI index, quantified the ecological quality of Beijing by combining the principal component analysis with the random forest algorithm, and analyzed the relationship between the RSEI and the four ecological indicators. Yuan (Yuan et al., 2021) and Xiong (Xiong et al., 2021) respectively inverted the ecological quality of Dongting Lake Basin and Erhai Basin based on RSEI, and Zheng (Zheng et al., 2020) evaluated the long-term ecological status of China's coastal areas based on RSEI. Xu (Xu et al., 2018)explored the relationship between impervious surface and RSEI to explore the connection between population growth and impervious surface, and fitted the model to predict the coming population and the ecological impact of impervious surface growth in Xiong'an New Area.

The long-term coal mining in Shanxi Province has caused serious pollution to the local ecological environment. Based on the characteristics of the main sources of ecological pollution in Shanxi Province, this paper uses the PCA method to couple the four ecological indicators of greenness, humidity, heat and dryness to obtain a comprehensive ecological quality index that reflects the ecological status of Shanxi Province. This index is used to monitor the land ecological status of Shanxi Province for a long time, periodically and comprehensively, It can provide scientific basis for the local government to formulate ecological restoration and protection policies.

2. MATERIALS AND METHODS

2.1 Study area

Shanxi Province is located on the east bank of the middle reaches of the Yellow River and on the Loess Plateau to the west of the North China Plain. It is bounded by Taihang Mountain in the east and adjacent to Hebei; Shaanxi and Henan are bordered by the Yellow River in the west and south, and Inner Mongolia is bordered by the Great Wall beyond the north, between 34 ° 34 ′ - 40 ° 44 ′ north latitude and 110 ° 14 ′ - 114 ° 33 ′ east longitude, with a total area of 156700 square kilometers. Shanxi Province has complex geomorphic types, including mountains, hills, platforms and plains. Mountains and hills account for 80% of the total area of the province, while plains and valleys account for 20% of the total area. Most areas of the province are above 1500 meters above sea level. This area belongs to temperate continental monsoon climate zone. In recent years, the annual precipitation of Shanxi Province has increased year by year.

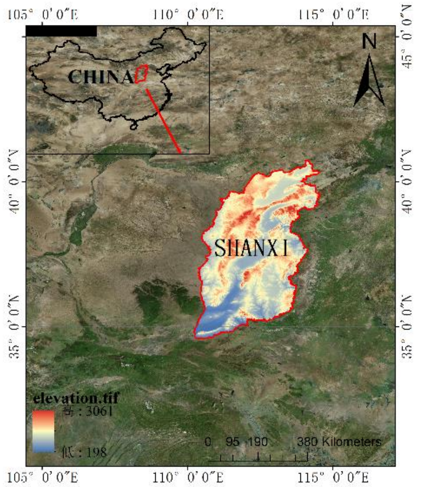

Figure 1. Location and the elevation of Shanxi Province.

2.2 Data and Pre-processing

The GEE platform is used to collect and process Landsat8OLI/TIRS images provided by the United States Geological Survey Center (USGS). In order to avoid the uncertainty caused by seasonal changes, the Landsat8 Collection2Level 2 surface reflectance data with cloud content less than 10% in the winter of 2014 to 2020 is screened. The data has been subject to radiation correction, atmospheric correction and other operations. In addition, the precipitation and temperature data are from the fifth generation reanalysis data (ERA-5), the digital elevation data are from the NASA-DEM dataset, and the GDP, the primary industrial output value, and the secondary industrial output value are from the statistical yearbook of Shanxi Province.

In the pre-processing stage, the Landsat8 satellite data was cloud masked by the mask function (CFMASK), and the water body was masked by the improved normalized water body index (MNDWI) (Xu, 2006). At the same time, era-5 data, NASA-DEM data, Shanxi Statistical Yearbook and other data are selected to study the driving factors of spatial and temporal changes of RSEI.

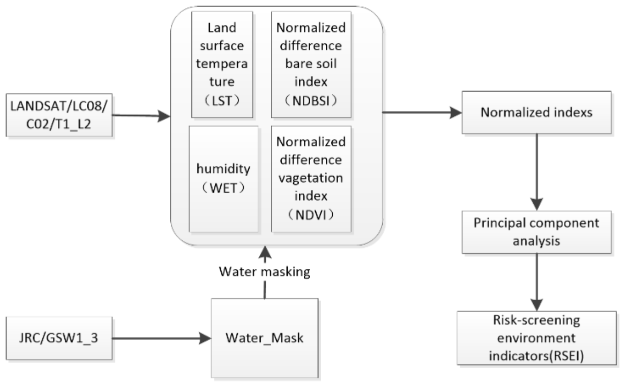

Figure 2. comprehensive risk assessment technology roadmap of Shanxi Province.

2.3 Methods

2.3.1 Construction of RSEI model: The comprehensive indicator RSEI based on the Pressure State Response (PSR) framework objectively assigns weights to the five indicators through PCA, avoiding the disadvantage of experts setting weights. In specific operation, NDVI represents greenness, and the third component of tassel cap transformation is humidity, LST represents heat, and NDBSI represents dryness. The calculated four indicators are respectively de outliers, normalized, and then linearly weighted to obtain the comprehensive indicator RSEI, in which the indicator weight is the feature vector corresponding to each feature value(Kim et al., 2021; Kotzee and Reyers, 2016). To sum up, the index has the advantages of objectivity, stability and visualization, and can quickly and scientifically express the surface ecological status.

The PCA is used to couple the information of the four ecological indicators, and the first principal component band with the highest contribution rate is selected for normalization to obtain the remote sensing ecological index (RSEI). The RSEI calculation formula is as follows:

$$RSEI_0 = f(NDVI, WET, NDBSI, LST) \ ;$$

$$RSEI = \frac{(RSEI_0 - RSEI_{0_{min}})}{(RSEI_{0_{max}} - RSEI_{0_{min}})} \ , \quad (1)$$

Among them, $RSEI_0$ represents the remote sensing ecological index before normalization, and $RSEI$ represents the remote sensing ecological index after normalization. According to the interval of 0.2, the RSEI values are divided into five categories: poor (0-0.2), average (0.2-0.4), moderate (0.4-0.6), good (0.6-0.8) and excellent (0.8-1). The larger the RSEI value, the better the ecological environment.

2.3.2 Model index inversion: (1) Greenness： NDVI reflects the growth status and biomass indicators of surface vegetation, and is widely used in vegetation coverage research and crop growth monitoring (Li et al., 2022). Therefore, NDVI is used as the greenness index in this study. The calculation formula is as follows:

$$NDVI = (B2 - B1)/(B1 + B2) \ , \quad (2)$$

Where, B1 and B2 are the red band and near-infrared band of Landsat 8 products respectively.

(2) Dryness： With the intensification of urbanization and human activities, green space is gradually replaced by buildings and bare land, which leads to the reduction of urban vegetation coverage. With the combined effect of urban heat island effect and greenhouse effect, the dryness of the ground increases and the environmental conditions deteriorate. In order to measure the dryness of the surface, Hu and Xu's index based cumulative index (IBI) and soil index (SI) can be used to construct a standardized differential cumulative and bare soil index (NDBSI) to represent the dryness of RSEI. The calculation formula is as follows:

$$SI = ((B1 + B6) - (B2 + B3))/((B1 + B6) + (B2 + B3)) \ ;$$

$$IBI = (2 * \frac{B6}{B6+b2} - \left(\frac{B2}{B1+b2} + \frac{B4}{B4+b6}\right))/(2 * \frac{B6}{B6+b2} + \left(\frac{B2}{B1+b2} + \frac{B4}{B4+b6}\right)) \ ;$$

$$NDBSI = (SI + IBI)/2 \ , \quad (3)$$

Where, B1-6 is the red band, near infrared band, blue band, green band and mid infrared band 1 of Landsat8 product respectively.

(3) Humidity： The tassel cap transformation generates three components: humidity, greenness and brightness. The third component of humidity can reflect the ground water content. In addition, large areas of water have a great impact on the humidity index. Generally, the water mask operation is performed before calculating the humidity. The humidity component is calculated as follows:

$$\mathrm{WET} = \mathrm{B1} * 0.1147 + \mathrm{B2} * 0.2489 + \mathrm{B3} * 0.2408 + \mathrm{B4} * 0.3132 - 0.3122 * \mathrm{B5} - 0.6416 * \mathrm{B6} - 0.5087 * \mathrm{B7} \ , \quad (4)$$

Where, B1~7 are respectively the red band, near infrared band, blue band, green band, mid infrared band 1 and mid infrared band 2 of Landsat8 products.

(4) Heat： Temperature reflects the heat index of a region and affects the exchange of sensible and latent heat between the ground, atmosphere and water body. It is a very important ecological indicator in the ecological environment. As the surface temperature is difficult to obtain, this study uses the temperature product Landsat8 launched by NASA to replace it. This product reflects the land surface temperature, with a time resolution of 16 days and a spatial resolution of 1000m, and is widely used in land ecological environment monitoring.

2.3.3 Spatial autocorrelation analysis: According to the first law of geography: "Everything is related to other things, but things near are more relevant than things far away.". In order to explore the spatial distribution of ecosystem monitoring results, this paper uses spatial autocorrelation to test whether RSEI is related to its adjacent spatial RSEI. The spatial correlation of RSEI was analyzed by Moran index and local Moran index. The global Moran index reflects the correlation of adjacent spatial values in the global range. The value range of the index is - 1~1. Negative numbers represent negative correlation and positive numbers represent positive correlation. The closer the absolute value of the Moran index is to 1, the stronger the spatial autocorrelation of the attribute values in the region is. The calculation formula is as follows:

$$Globalmoran'sI = \frac{m * \sum_{i=1}^{m} \sum_{j=1}^{m} W_{ij}(D_i - \bar{D})(D_j - \bar{D})}{\sum_{i=1}^{m} \sum_{j=1}^{m} W_{ij}(D_i - \bar{D})^2} \ , \quad (5)$$

After the global Moran index calculates that the study area has spatial autocorrelation, the local Moran index can be used to analyze whether the study area has spatial heterogeneity. If there is no global spatial correlation, the local Moran index can also be used to find the area with local spatial autocorrelation. The calculation formula is as follows:

$$Lobalmoran'sI = \frac{(D_i-\bar{D})*\sum_{j=1}^{m} W_{ij}(D_j-\bar{D})}{\sum_{i=1}^{m}(D_i-\bar{D})^2} \quad , \quad (6)$$

Where, m is the total number of pixels, D_i and D_j respectively represent the RSEI at location i and j, $\bar{D}$ represents the average value of RSEI in the study area, and W_{ij} represents the spatial weight.

2..3.4 Geodetector: Geographic detectors include factor detectors, interaction detectors, risk detectors, and ecological detectors. This paper uses geographic detectors to study the spatial differentiation of six factors, elevation, slope, greening, humidity, dryness, and heat, and Shanxi the variance of the total region, then it can be RSEI. The principle is that the spatial distribution of independent variables and dependent variables should be consistent. If the variance of a sub region is less than considered that there is spatial differentiation in the region.
The q value of the factor detector indicates the relative importance of the factor to RSEI in the study area. The greater the q value, the greater the importance of the factor. This method can be used to determine the driving factors of ecological quality in Shanxi Province. The calculation formula of q value is as follows:

$$q = 1 - \frac{\sum_{j=1}^{M} N_j \sigma_j^2}{N\sigma^2} \qquad (7)$$

Where N_j and σ_j^2 are the sample number and variance of the factor labeled j, N and σ^2 are the sample number and variance of the dependent variable in the whole study area.

3. RESULTS

3.1 RSEI

As shown in Figure 3, The seven years' RSEI results from 2013 to 2019 are classified using 0.2 interval, that is, 0-0.2 is Class 1 (Poor), 0.2-0.4 is Class 2 (Fair), 0.4-0.6 is Class 3 (Moderate), 0.6-0.8 is Class 4 (Good), and 0.8-1 is Class 5 (Excellent). The classification display is shown in Figure 3. It can be seen from the figure that most of the regions in 2013-2014 fall into two categories: Category 2 and Category 3. Since 2015, Category 3 has decreased significantly, and Category 2 has occupied a large area of Shanxi Province. In 2015, there were 5 types in the north. In 2016-2017, 2 types occupied most of the area. In 2018, the north began to recover 3 types, sometimes 4 or 5 types. It can be seen from the winter mean value table in Figure 4 that the two years 2013-2014 were the highest value of RSEI in Shanxi Province. In winter 2015, RSEI dropped sharply, and after 2015, it showed a slow rise.

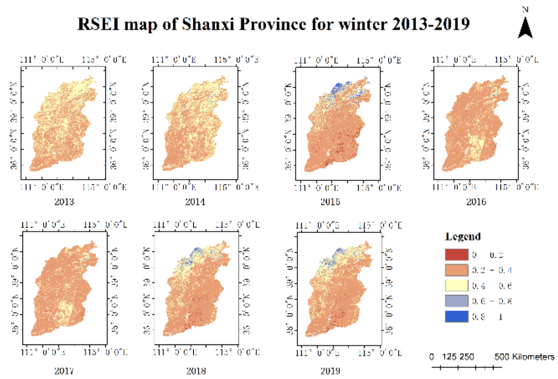

Figure 3. RSEI map of Shanxi Province for winter 2013-2019

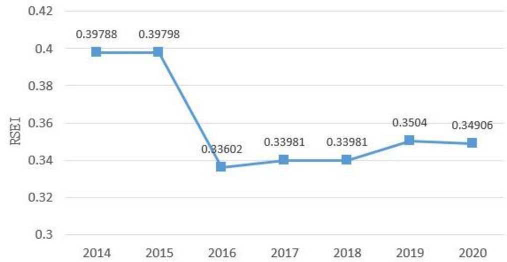

Figure 4. Average curve of RSEI of Shanxi Province for winter

3.2 Spatial autocorrelation

In order to reflect the global spatial distribution pattern as much as possible, this paper uses fishing nets to sample the seven year winter RSEI results to obtain 1506 sampling points, and extracts the corresponding RSEI values of the sampling points for spatial distribution pattern analysis. Specifically, the invalid values of the sampled RSEI values are eliminated, and the global and local autocorrelation of the sampled RSEI values are analyzed using spatial autocorrelation. The results are as Table 1.

Year	Moran'I	P	z	Correlation
2013	0.23	0	8.59	positive
2014	0.28	0	10.6	positive
2015	0.5	0	25.0	positive
2016	0.36	0	13.6	positive
2017	0.36	0	13.4	positive
2018	0.51	0	26.0	positive
2019	0.54	0	27.0	positive

Table 1. spatial autocorrelation of Shanxi Province

It can be seen from Table 1 that the spatial autocorrelation P values in the seven years from 2013 to 2019 are all 0, so the null hypothesis is rejected, that is, the spatial pattern presented by the data has a significant spatial structure, and the z scores are far greater than 2.58 in the seven years, that is, the probability of randomly generating this cluster pattern is less than 1%, and the Moran index is greater than 0, and the RSEI shows a positive spatial correlation in Shanxi Province. The spatial aggregation result obtained by using local spatial autocorrelation is shown as Figure 5.

https://doi.org/10.5194/isprs-archives-XLVIII-3-W1-2022-59-2022 | © Author(s) 2022. CC BY 4.0 License.

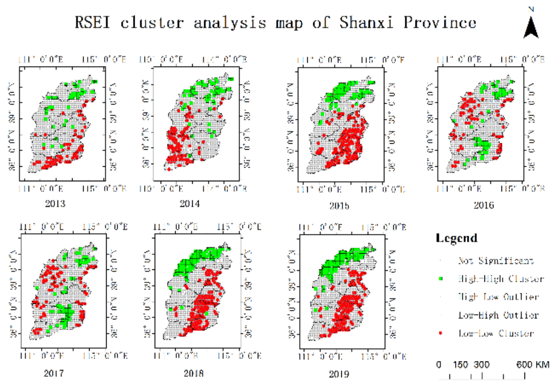

Figure 5. Geodetector results of Shanxi for 2013-2019

It can be seen from the above figure that in 2014, the low value of 2016,2019,2020 was concentrated in the southeast, while the northwest was more concentrated in the high value. The high value in 2017,2018 is mainly distributed in the middle of the province, while the low value is closer to the junction of Shaanxi and Hebei. In 2015, low values were mainly distributed in the southwest, while high values were distributed in the north of Shanxi Province. From the attribute value statistics table in the following table, it can be seen that the number of high value clusters in 2014-2020 is generally increasing year by year, with a sharp increase in 2016. The low value aggregation statistical value is relatively irregular, increasing year by year in 2014-2016 and then decreasing, and the number of low values and high values in 2017-2020 have similar increase and decrease laws. It can be seen from Figure 4 that the overall trend of high value aggregation is rising, and it should also be noted that low value aggregation has a consistent trend of change.

3.3 Geodetector

The factor detector results for 2013-2019 are as follows：

	2013	2014	2015	2016	2017	2018	2019
dem	N	Y	Y	N	N	Y	Y
tem	N	Y	Y	Y	Y	Y	Y
water	N	N	Y	N	N	Y	Y
gdp	Y	Y	Y	Y	Y	Y	Y
no1	Y	Y	Y	Y	Y	Y	Y
no2	Y	Y	Y	Y	Y	Y	Y

Table 2. Geodetector results of Shanxi Province for 2013-2019

4. CONCLUSION

There are two different trends in the north and southeast of Shanxi Province. The RSEI in the north is high value aggregation in spatial mode, while the RSEI in the southeast is low value aggregation in spatial mode. From the perspective of administrative region, northern Shanxi is the traditional coal mining area of Datong City. As a "resource-based city", Datong takes coal mining as the leading industry. After the early predatory mining, the single industrial structure tends to collapse. In 2005, it was reported that Datong is facing a situation of resource depletion. The time range selected in this study is 2013-2019. Datong City changes its industrial structure after resource depletion, The ecological environment has been restored to a certain extent. With the growth of time, the high value of RSEI has gathered here.

REFERENCES

Gao, B.C., 1996. NDWI - A normalized difference water index for remote sensing of vegetation liquid water from space. REMOTE SENSING OF ENVIRONMENT, 58(3): 257-266.

Gao, P.W. et al., 2020. Evaluation of the Temporal and Spatial Changes of Ecological Quality in the Hami Oasis Based on RSEI. SUSTAINABILITY, 12(18).

Garaba, S.P., Friedrichs, A., Voss, D. and Zielinski, O., 2015. Classifying Natural Waters with the Forel-Ule Colour Index System: Results, Applications, Correlations and Crowdsourcing. INTERNATIONAL JOURNAL OF ENVIRONMENTAL RESEARCH AND PUBLIC HEALTH, 12(12): 16096-16109.

Hang, X., Li, Y.C., Luo, X.C., Xu, M. and Han, X.Z., 2020. Assessing the Ecological Quality of Nanjing during Its Urbanization Process by Using Satellite, Meteorological, and Socioeconomic Data. JOURNAL OF METEOROLOGICAL RESEARCH, 34(2): 280-293.

KAUFMAN, Y.J. and TANRE, D., 1992. ATMOSPHERICALLY RESISTANT VEGETATION INDEX (ARVI) FOR EOS-MODIS. IEEE TRANSACTIONS ON GEOSCIENCE AND REMOTE SENSING, 30(2): 261-270.

Keyantash, J.A. and Dracup, J.A., 2004. An aggregate drought index: Assessing drought severity based on fluctuations in the hydrologic cycle and surface water storage. WATER RESOURCES RESEARCH, 40(9).

Kim, J.E., Yu, J., Ryu, J.H., Lee, J.H. and Kim, T.W., 2021. Assessment of regional drought vulnerability and risk using principal component analysis and a Gaussian mixture model. NATURAL HAZARDS, 109(1): 707-724.

Kotzee, I. and Reyers, B., 2016. Piloting a social-ecological index for measuring flood resilience: A composite index approach. ECOLOGICAL INDICATORS, 60: 45-53.

Li, Y.D., Li, Z.J., Wang, J.J. and Zeng, H., 2022. Analyses of driving factors on the spatial variations in regional eco-environmental quality using two types of species distribution models: A case study of Minjiang River Basin, China. ECOLOGICAL INDICATORS, 139.

Lu, D.S. et al., 2016. A survey of remote sensing-based aboveground biomass estimation methods in forest ecosystems. INTERNATIONAL JOURNAL OF DIGITAL EARTH, 9(1): 63-105.

Mildrexler, D.J., Zhao, M.S. and Running, S.W., 2009. Testing a MODIS Global Disturbance Index across North America. REMOTE SENSING OF ENVIRONMENT, 113(10): 2103-2117.

Ren, W., Zhang, X.S. and Peng, H.J., 2022. Evaluation of Temporal and Spatial Changes in Ecological Environmental Quality on Jianghan Plain From 1990 to 2021. FRONTIERS IN ENVIRONMENTAL SCIENCE, 10.

Rhee, J., Im, J. and Carbone, G.J., 2010. Monitoring agricultural drought for arid and humid regions using multi-sensor remote sensing data. REMOTE SENSING OF ENVIRONMENT, 114(12): 2875-2887.

Singh, K.V., Setia, R., Sahoo, S., Prasad, A. and Pateriya, B., 2015. Evaluation of NDWI and MNDWI for assessment of waterlogging by integrating digital elevation model and groundwater level. GEOCARTO INTERNATIONAL, 30(6): 650-661.

Tang, P.L. et al., 2021. Local and telecoupling coordination degree model of urbanization and the eco-environment based on RS and GIS: A case study in the Wuhan urban agglomeration. SUSTAINABLE CITIES AND SOCIETY, 75.

Xiong, Y. et al., 2021. Assessment of spatial?temporal changes of ecological environment quality based on RSEI and GEE: A case study in Erhai Lake Basin, Yunnan province, China. ECOLOGICAL INDICATORS, 125.

Xu, H.Q., 2006. Modification of normalised difference water index (NDWI) to enhance open water features in remotely sensed imagery. INTERNATIONAL JOURNAL OF REMOTE SENSING, 27(14): 3025-3033.

Xu, H.Q. et al., 2018. Prediction of ecological effects of potential population and impervious surface increases using a remote sensing based ecological index (RSEI). ECOLOGICAL INDICATORS, 93: 730-740.

Xu, H.Q., Wang, Y.F., Guan, H.D., Shi, T.T. and Hu, X.S., 2019. Detecting Ecological Changes with a Remote Sensing Based Ecological Index (RSEI) Produced Time Series and Change Vector Analysis. REMOTE SENSING, 11(20).

Yang, L., Qian, F., Song, D.X. and Zheng, K.J., 2016. Research on Urban Heat-island Effect. FOURTH INTERNATIONAL CONFERENCE ON COUNTERMEASURES TO URBAN HEAT ISLAND, (UHI 2016), 169, 11-18 pp.

Yang, X.Y., Meng, F., Fu, P.J., Zhang, Y.X. and Liu, Y.H., 2021. Spatiotemporal change and driving factors of the Eco-Environment quality in the Yangtze River Basin from 2001 to 2019. ECOLOGICAL INDICATORS, 131.

Yuan, B.D. et al., 2021. Spatiotemporal change detection of ecological quality and the associated affecting factors in Dongting Lake Basin, based on RSEI. JOURNAL OF CLEANER PRODUCTION, 302.

Yue, H., Liu, Y., Li, Y. and Lu, Y., 2019. Eco-Environmental Quality Assessment in China's 35 Major Cities Based On Remote Sensing Ecological Index. IEEE ACCESS, 7: 51295-51311.

Zheng, Z.H., Wu, Z.F., Chen, Y.B., Yang, Z.W. and Marinello, F., 2020. Exploration of eco-environment and urbanization changes in coastal zones: A case study in China over the past 20 years. ECOLOGICAL INDICATORS, 119.